Simplifying the fabrication of n-PERT solar cells: Recent progress at ISFH

Bianca Lim[1], **Fabian Kiefer**[1], **Nadine Wehmeier**[1], **Till Brendemühl**[1], **Yevgeniya Larionova**[1], **Frank Heinemeyer**[1], **Jan Krügener**[2], **Robby Peibst**[1] & **Thorsten Dullweber**[1]

[1]Institute for Solar Energy Research Hamelin (ISFH), Emmerthal; [2]Institute of Electronic Materials and Devices, Leibniz University of Hanover, Germany

ABSTRACT

In this paper large-area (239cm^2) n-type passivated emitter, rear totally diffused (n-PERT) solar cells are compared with state-of-the-art p-type passivated emitter and rear cells (p-PERC) to evaluate potential advantages of n-PERT over p-PERC. In particular, an investigation has been carried out of fully screen-printed bifacial n-PERT solar cells, in which the boron-doped emitter is contacted with aluminium-containing silver (AgAl) pastes, as well as of n-PERT back-junction (BJ) solar cells, in which the B-doped emitter is locally contacted with screen-printed Al. Using two separate quartz furnace diffusions for the B- and P-doped regions, efficiencies of up to 20.3% on bifacial n-PERT solar cells and of up to 20.5% on n-PERT BJ solar cells were achieved. In comparison, reference p-PERC solar cells that were processed in parallel achieved efficiencies of up to 20.6% before light-induced degradation (LID), but degraded to 20.1% after 48 hours of illumination. In addition, ion implantation and pre-deposition of dopant sources have been evaluated as alternative technologies for forming the full-area doping of the front and rear wafer surfaces, thus reducing the number of processing steps for n-PERT solar cells. Using ion implantation and a co-annealing step, efficiencies of up to 20.6% for bifacial n-PERT solar cells have been achieved, and of up to 20.5% for n-PERT solar cells, in which the P-doped back-surface field is contacted with evaporated Al. By employing a boron silicate glass (BSG) deposited via plasma-enhanced chemical vapour deposition (PECVD) as a dopant source, along with a co-diffusion step, n-PERT BJ solar cells have been fabricated with up to 19.8% energy conversion efficiency.

Introduction

The majority of crystalline silicon solar cells are currently fabricated on boron-doped (B-doped) p-type silicon. However, forecasts – such as the ITRPV Roadmap [1] – predict that the share of phosphorus-doped (P-doped) n-type silicon will increase in coming years. One advantage of P-doped n-Si is the absence of light-induced degradation (LID) of the carrier lifetime, which is associated with the simultaneous presence of boron and oxygen in p-Si [2]. In addition, the most common metal impurities – such as iron – are less harmful in n-Si, resulting in significantly higher minority-carrier lifetimes in n-type Czochralski-grown silicon (Cz-Si) [3]. As a consequence, high-efficiency solar cell concepts – such as interdigitated back-contact (IBC) or silicon heterojunction (HJT) cells – often use n-Si wafers [4,5].

> "Forecasts predict that the share of phosphorus-doped (P-doped) n-type silicon will increase in coming years."

With regard to upgrading existing production lines for screen-printed p-type silicon solar cells to production lines for n-Si solar cells, the IBC and HJT technologies both use processing tools which are different from those for standard p-type solar cells, and which potentially require a rather large investment in new equipment. The n-type passivated emitter, rear totally diffused (n-PERT) or passivated emitter, rear locally doped (PERL) concepts, on the other hand, use similar processing steps and tools to those for standard p-type solar cells, and hence should require only little, if any, tool-conversion investment.

A number of variations of the n-PERT solar cell have been proposed. Laboratory-type small-area cells (4cm^2) with a B-doped front-side emitter and a P-doped back-surface field (BSF) have achieved efficiencies of up to 22.7% [6], demonstrating the high efficiency potential of the n-PERT concept. A more industrially feasible alternative is a screen-printed bifacial structure, which is shown schematically in Fig. 1(a). The bifacial n-PERT solar cell has already been commercialized [7] and is currently the most intensively studied n-PERT structure [8–10]. Both sides of the solar cell are textured and the two highly doped regions may be contacted via screen printing, in which silver (Ag) pastes are used for the P-doped BSF and aluminium-containing Ag pastes (AgAl) are used to contact the B-doped emitter. Efficiencies of up to 20.5% have been reported for an ion-implanted, fully screen-printed 239cm^2 solar cell utilizing this structure [10].

Besides the advantage of a potentially lean process flow, the bifacial n-PERT concept could offer the advantage of harvesting additional light from the rear side, which may result in an enhanced energy yield. A potential disadvantage of this structure is that silver consumption is higher than that for a standard p-type solar cell, most of the rear side of which is metallized by screen-printed Al. One possible method of reducing Ag consumption is the deposition of Al via physical vapour deposition (PVD) on the rear side [11,12], as shown in Fig. 1(b). Another possibility is an n-PERT back-junction (BJ) solar cell, since the B-doped emitter, in contrast to the P-doped BSF, can also be contacted with screen-printed Al paste; a schematic of the structure is shown in Fig.1(c). The n-PERT BJ solar cell has a strong resemblance to a p-type passivated emitter and rear cell (p-PERC), both in architecture and in processing sequence, potentially facilitating its implementation in p-PERC production lines. The usage of AgAl paste to contact B-doped emitters can also result

ASYS SOLAR

Laser Contact Opening

Inline System

Laser Island

Contact Opening (LCO) of All Dielectric Layers

- Unique to the market: fully integrable into metallization lines
- High-precision: market-leading repeatability of wafer positioning
- Throughput of up to 3600 cph on dual lane

ASYS SOLAR Laser Solutions

ASYS offers laser systems for different processes. All laser systems are based on a platform concept. They provide proven quality and can be upgraded easily. In combination with an ASYS loader and unloader, the systems can be transformed into laser islands (single lane / dual lane). For some processes they can also be integrated directly into the metallization line.

ASYS GmbH
Benzstrasse 10, 89160 Dornstadt, Germany

www.asys-solar.com

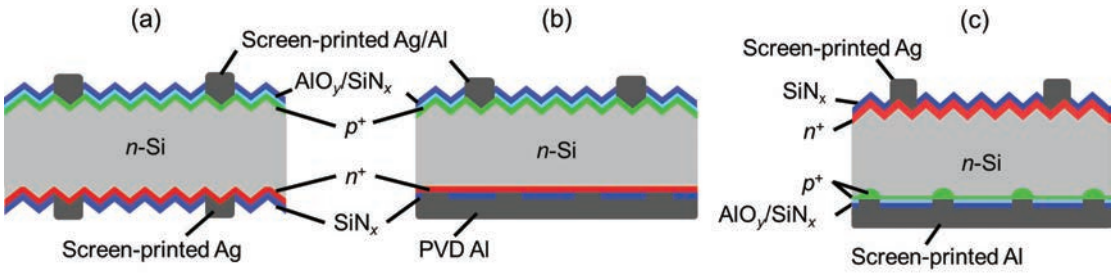

Figure 1. Schematics of (a) bifacial n-PERT solar cell; (b) front-junction n-PERT solar cell with evaporated Al on the rear side; and (c) n-PERT BJ solar cell. The Al on the rear side can be either evaporated or screen printed.

in significant V_{oc} losses [13], which would be avoided in the n-PERT BJ concept. Indeed, the highest large-area (239cm^2) n-PERT efficiency reported so far of 21.3% was achieved with an n-PERT BJ solar cell featuring PVD Al rear-side metallization [14]. For a fully screen-printed version of this cell concept, a maximum efficiency of 20.7% has been reported so far [14].

The n-PERT structure can be modified to create an n-PERL structure, in which only localized P-doped regions are formed. In this case, the wafer itself has to provide a certain lateral conductivity for the electrons, which implies stronger restrictions on the base resistivity than for the n-PERT concept. However, one advantage of the n-PERL concept is the decoupling of the doping level required for low contact resistance in the metallized regions from the level required for low Auger and Shockley-Read-Hall surface recombination in the passivated regions.

A major manufacturing challenge of the n-PERT solar cell is the formation of two different full-area highly doped regions at the front and rear wafer surfaces. In laboratory processing, a popular method is to use two separate quartz furnace diffusions, where dielectric layers are used as diffusion barriers. However, since these layers are sacrificial, this processing sequence is rather complex for production; alternative doping techniques might thus be required in order to successfully transfer n-PERT technology to mass production.

In this paper, two doping techniques for achieving different front- and rear-surface diffusions are discussed: 1) ion implantation, and 2) doping from a pre-deposited boron-containing silicon oxide layer (boron silicate glass – BSG). Both techniques are inherently single sided and may be optimized to require only one high-temperature step. Saturation current densities J_{0e} of the resulting B-doped regions are reported as well as the energy conversion efficiencies of solar cells which were fabricated using these techniques. Regarding the investigated cell concepts, recent R&D results of n-PERT front-junction structures (either bifacial or with PVD Al rear-side metallization), n-PERT BJ and n-PERL solar cells are presented. When sequential quartz furnace diffusions are used, energy conversion efficiencies of up to 20.5% for n-PERT BJ solar cells are achieved. With ion implantation and a co-annealing step, the efficiencies achieved are up to 20.6% for fully screen-printed bifacial n-PERT cells and up to 20.5% for n-PERT cells with PVD metallization of the P-BSF.

Reference n-PERT solar cells using two separate diffusions

To evaluate the potential of new processing technologies such as ion implantation and pre-deposition of dopant sources, two reference processing sequences are established, one for bifacial n-PERT solar cells and the other for n-PERT BJ solar cells. Both reference processes use two separate quartz furnace diffusions and the application of dielectric protection layers to form the two different full-area doped regions on the front and rear sides of the wafer. In addition, both reference processes use screen printing to contact both the front and rear sides of the solar cell.

For the bifacial solar cells, P-doped Cz-Si wafers with a resistivity of 5–6Ω·cm and an area of 239cm^2 are used. The processing sequence includes saw damage removal in KOH, alkaline texturing of the front and rear surfaces, a BBr_3 boron diffusion, a $POCl_3$ phosphorus diffusion, and the application of sacrificial dielectric layers prior to the two separate diffusions. The P-doped rear side of the solar cell is passivated with plasma-enhanced chemical vapour deposited (PECVD) silicon nitride (SiN_x), while the B-doped front side is passivated with a stack of atomic layer deposited (ALD) aluminium oxide (AlO_y) and PECVD SiN_x. After passivation, AgAl paste is screen printed on the B-doped emitter and Ag paste on the P-doped BSF.

Since AgAl pastes can induce high recombination on B-doped emitters [13], an evaluation of the dual-print technique for reducing the contact area of the AgAl paste with the B-doped emitter was also performed. Dual print uses a thin nickel foil as a stencil to print the contact fingers, while the busbars are printed with a conventional mesh screen. The advantage of stencil printing is that no obstructions are present in the openings, resulting in a much more homogeneous Ag finger height compared with that obtained in screen printing. At the same time, the busbars and fingers are printed in two separate steps. Although the number of processing steps is increased, dual print offers the opportunity to use two different pastes for the fingers and the busbars, and, in particular, a non-firing-through busbar paste. As a result, the area fraction of the potentially highly recombination-active AgAl contact was reduced from 7.4% to 4.1%.

The use of single screen printing for fingers and busbars has led to the realization of energy conversion efficiencies of up to 20.0% for bifacial n-PERT solar cells using two separate diffusions (measured on a reflecting chuck). With dual print, and thus non-contacting busbar pastes, energy conversion efficiencies of up to 20.3% (independently measured at Fraunhofer ISE CalLab on a reflecting chuck) have been achieved.

The reference processing sequence of n-PERT BJ solar cells is based on the high-efficiency p-PERC process detailed in Hannebauer et al. [15]. Processing steps include saw damage removal in KOH, BBr_3 boron diffusion, deposition of a dielectric layer on the rear side of the wafer, alkaline texturing (thus removing the B-doped region on the front side), $POCl_3$ phosphorus diffusion, and subsequent removal of the protection layer and phosphosilicate glass (PSG) in HF. The P-doped front side of the solar cell is passivated with PECVD SiN_x, while the B-doped rear side is passivated with a stack of ALD AlO_y and PECVD SiN_x. In order to facilitate the formation of the rear contact, the AlO_y/SiN_x stack on the rear is locally ablated (line shaped) using a picosecond

	Co-diffusion using PECVD BSG layers	Ion implantation with subsequent co-annealing
Advantages	+ Independent tailoring of P and B profile possible + Co-diffusion utilizes conventional $POCl_3$ tubes + PECVD BSG layer might be multi-functional (e.g. doping source/diffusion barrier and protection layer for single-side texturing)	+ High efficiencies up to 22.7% already demonstrated [6] + Excellent homogeneity + Silicon oxide passivation might be grown in situ during anneal + Selective emitter realizable via shadow masks + Selective BSF (PERL structure) realizable via shadow masks + (Front junction): AgAl metallization-induced V_{oc} loss less pronounced than for BBr_3 diffusion [11,17] + Edge isolation via masked implant (no additional step)
Disadvantages	- Edge isolation possibly required - Local doped structures (selective emitter, selective BSF) more challenging to realize	- Co-anneal (high temperature budget required for B anneal) complicates tailoring of P profile

Table 1. Potential advantages and disadvantages of co-diffusion using PECVD BSG layers and of ion implantation with subsequent co-annealing.

laser with a wavelength of 532nm before screen printing Ag on the front side and Al on the rear. Finally, the solar cells are co-fired. With the reference process, energy conversion efficiencies of up to 20.5% (independently measured at Fraunhofer ISE CalLab) [16] have been achieved so far.

Technologies for simplifying the n-PERT process

In parallel with the establishment of n-PERT baseline processes based on two separate quartz furnace diffusions (BBr_3 and $POCl_3$), two technologies that potentially lead to a significant process simplification of the n-PERT were evaluated: 1) co-diffusion using PECVD BSG layers as a boron source, and 2) ion implantation of boron and phosphorus, with a subsequent co-anneal of the implant damage. The potential advantages and disadvantages of both technologies are listed in Table 1 (as research institutes, we cannot comment on cost issues or on tool-related challenges).

In the case of ion implantation, several investigative groups have solved the challenge of annealing the damage induced by the non-amorphizing implant of elementary boron [12,17–20]. In the work reported in this paper, implanted boron was furnace annealed at 1050°C [12]. For p^+ sheet resistances in the range 50–100Ω/sq. on textured surfaces, saturation current densities J_{0e} of 50–80fA/cm^2 are obtained using fired AlO_y/SiN_x stacks for passivation, as shown in Fig. 2 [12]. These values, since they are as low as those obtained for BBr_3-diffusion-based B-doped emitters, indicate a sufficient annealing of implant-induced crystal defects [21].

However, during the co-annealing of B and P implants, the relatively high temperature budget required for the B anneal results in deep P profiles with low peak- and surface-doping concentrations.

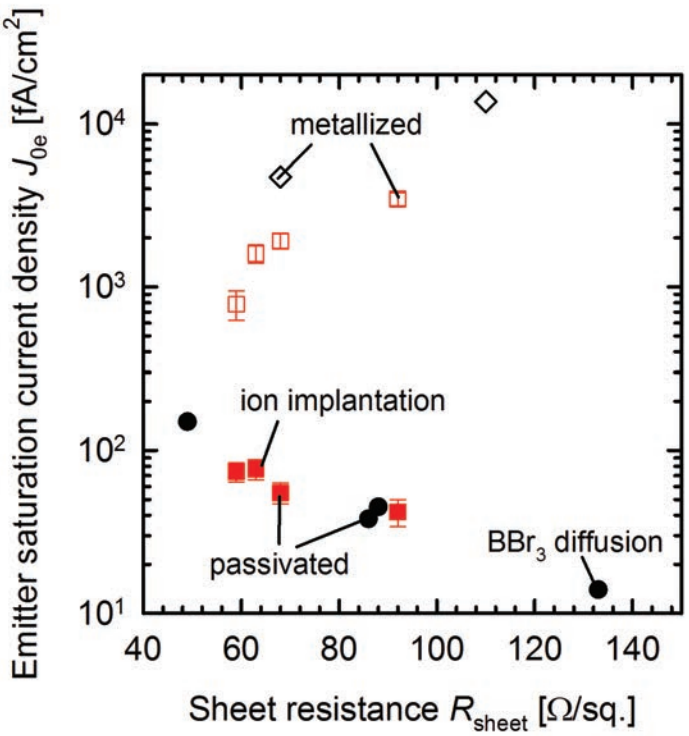

Figure 2. Emitter saturation current densities J_{0e} as a function of sheet resistance R_{sheet} on textured surfaces. Black symbols denote values for boron-diffused emitters [22,23], whereas red symbols correspond to ion implantation. Open symbols refer to metallized surfaces, and filled symbols represent passivated surfaces (fired AlO_y/SiN_x stack).

Thus, achieving low specific contact resistances with Ag screen printing on the n^+ doped regions is not trivial, although this is less of an issue because of recent Ag paste improvements. In any case, the solution is to use a sufficiently high P dose. Alternatively, PVD metallization of the n^+ doped regions also yields low specific contact resistances for relatively low surface-doping concentrations of ~10^{19}cm^{-3} [24].

For the ion-implanted and co-annealed bifacial n-PERT solar cells, a double-side texture is applied after initial wafer cleaning. A B implant on the front side and a P implant on the rear are then performed, followed by a co-annealing step. Similarly to the reference process, the rear side is passivated with PECVD SiN_x and the front side with an ALD-AlO_y/PECVD-SiN_x stack. For contacting, AgAl paste is printed on the B-doped emitter and Ag paste on the P-doped BSF. Contact formation is done in a co-firing step. Sufficiently low specific contact resistances on the P-doped BSF are obtained, even for moderate P doses, by using state-of-the-art Ag screen-printing pastes. The highest independently confirmed efficiency of 20.3% for these types of cell is identical

to that for the $BBr_3/POCl_3$-diffusion-based bifacial n-PERT reference (Table 2). With further improvements, an in-house measured efficiency of 20.6% was recently achieved for ion-implanted, co-annealed and fully screen-printed bifacial n-PERT cells (Table 2).

"Sufficiently low specific contact resistances on the P-doped BSF are obtained, even for moderate P doses, by using state-of-the-art Ag screen-printing pastes."

PVD Al for contacting the P-doped BSF was also evaluated; in this case, the solar cells are only textured on the front side. After printing AgAl paste on the B-doped emitter, the solar cells are fired. Subsequently, the SiN_x on the rear side is locally ablated (point shaped) using a picosecond laser with a wavelength of 532nm, and the Al is evaporated. Finally, a short contact tempering [12] is performed. As in the case of the reference bifacial solar cells, standard screen printing of the front-side AgAl metallization was compared with dual printing using a non-contacting Ag paste for the busbars. With single screen printing, energy conversion efficiencies of up to 20.3% and a V_{oc} of 663mV were achieved; the use of dual print resulted in efficiencies of up to 20.5% and a V_{oc} of 665mV (Table 2).

Interestingly, it was observed that state-of-the-art commercial AgAl pastes induce a V_{oc} loss of only ~10mV for the ion-implanted n-PERT solar cells. This is much less than the 20–30mV reported for screen-printed metallization of BBr_3 diffused emitters [13]; this was also observed for the reference bifacial n-PERT solar cells. One possible reason for this finding is the slightly different shape of the B profiles after diffusion and after implant.

Table 2 also compares the characteristics of the reference n-PERT BJ solar cells (fabricated using two separate diffusions) with the characteristics of p-PERC solar cells, which were processed in parallel. The p-PERC solar cells used 3Ω·cm B-doped Cz-Si, which exhibits the well-known LID of the minority-carrier lifetime and thus the solar cell efficiency. As a result, the initial energy conversion efficiency of 20.6% degrades to a final value of 20.1% after illumination for 48 hours. In contrast,

	η [%]	J_{sc} [mA/cm^2]	V_{oc} [mV]	*FF* [%]
Reference bifacial n-PERT	20.3*	38.6*	658*	80.0*
Ion-implanted bifacial n-PERT	20.3*	38.8*	656*	79.9*
Ion-implanted n-PERT, PVD rear side	20.5*	38.8*	665*	79.5*
Ion-implanted bifacial n-PERT (late-news result)	20.6	38.9	662	79.9
Reference n-PERT BJ	20.5*	38.7*	665*	79.8*
p-PERC, 3Ω·cm	20.6	38.9	661	80.1
p-PERC, 3Ω·cm (degraded)	20.1	38.8	657	79

*independently measured at ISE CalLab

Table 2. Performance characteristics of different n-PERT and p-PERC solar cells (239cm^2), which were fabricated using conventional quartz furnace diffusions as well as ion implantation by applying the process sequences of Table 3.

A: p-PERC	B: n-PERT BJ	C: bifacial n-PERT FJ using ion implantation	D: n-PERT FJ using ion implantation and PVD Al
Wafer cleaning	Wafer cleaning	Wafer cleaning	Wafer cleaning
Rear protection layer	B diffusion BSG etch Rear protection layer		Rear protection layer
Texturing	Texturing	Texturing	Texturing
P diffusion PSG+dielectric etch	P diffusion PSG+dielectric etch	Front: B implant Rear: P implant Co-annealing	Protection layer removal Front: B implant Rear: P implant Co-annealing
Rear: AlO_y/SiN_x Front: SiN_x	Rear: AlO_y/SiN_x Front: SiN_x	Rear: SiN_x Front: AlO_y/SiN_x	Rear: SiN_x Front: AlO_y/SiN_x
Rear: laser ablation	Rear: laser ablation		
Front: Ag screen printing	Front: Ag screen printing	Front: AgAl screen printing	Front: AgAl screen printing
Rear: Al screen printing	Rear: Al screen printing	Rear: Ag screen printing	
Co-firing	Co-firing	Co-firing	Firing
			Rear: laser ablation Rear: PVD Al Contact tempering
11 steps	13 steps	10 steps	14 steps

Table 3. Process sequences for the different solar cells.

the efficiency of the n-PERT BJ solar cells remains stable at 20.5% (±0.1% is measured, which is within the measurement uncertainty).

Apart from the resulting energy conversion efficiency, the number of processing steps is also an important characteristic of a solar cell process. Table 3 gives an overview of the process sequences as described above and indicates the steps performed for the fabrication of A) p-PERC solar cells; B) n-PERT BJ solar cells using two separate diffusions; C) bifacial n-PERT front-junction (FJ) solar cells using ion implantation; and D) n-PERT FJ solar cells with full-area PVD Al on the rear side. (Common processing steps are highlighted in blue.)

When compared with the process sequence for p-PERC solar cells, the process sequence for ion-implanted bifacial n-PERT FJ solar cells (C) already seems viable, whereas the process sequences B and D probably need process simplifications to become feasible. For the ion-implanted n-PERT FJ solar cells with PVD Al on the rear side (D), for example, one-sided texturing would reduce the number of process steps by two. For n-PERT BJ solar cells (B), single-side pre-deposition of dopant sources is a very interesting alternative, as it means one high-temperature step and one dielectric etch can be removed from the process sequence.

Different deposition techniques – such as spin-on [25], PECVD [26,27] and atmospheric pressure chemical vapour deposition (APCVD) [28] – are currently being investigated for such single-side pre-depositions. Efficiencies up to 19.3% have been achieved [25] using a printable boron source and screen-printed contacts, while 19.9% has been reported for a bifacial n-PERT solar cell using APCVD BSG as the dopant source [28].

In the study reported here, BSG layers deposited by PECVD using silane (SiH_4), nitrous oxide (N_2O) and diborane (B_2H_6) as precursor gases were evaluated. Fig. 3 shows the saturation current densities J_{0e} obtained for B-doped regions as a function of sheet resistance R_{sheet}. The use of PECVD BSG layers as the dopant source results in J_{0e} values of 40–60fA/cm² on planar surfaces for sheet resistances between 50 and 180Ω/sq. (passivated with annealed ALD AlO_y). These values are a factor of two to five higher than those reported for planar BBr_3 diffused samples passivated similarly (indicated by the black symbols); however, the difference is smaller at moderate sheet resistances around 90Ω/sq. In addition,

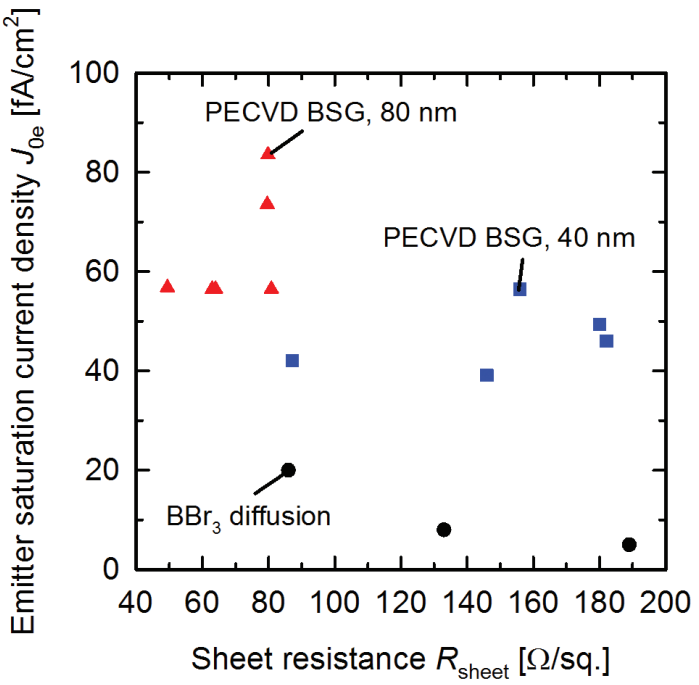

Figure 3. Emitter saturation current densities J_{0e} of boron diffusions on a planar surface passivated with annealed ALD AlO_y as a function of sheet resistance R_{sheet}. The black circles represent samples from BBr_3 diffusions [22], whereas the red triangles and blue squares correspond to samples that used PECVD BSG as the dopant source.

the sheet resistance of the PECVD BSG B diffusion is adjustable over a wide range by varying the composition and thickness of the PECVD BSG as well as the drive-in conditions [26,29]. When the BSG layer is deposited on the rear side of the solar cell after saw damage removal, it can also serve as a protection layer during the subsequent front-side texturing step. This multi-functionality further reduces process complexity, especially for n-PERT BJ solar cells.

> "Co-diffusion from doped oxides seems especially suited to n-PERT BJ solar cells."

The formation of the P-doped region can be done either with a P-containing silicon oxide (PSG) deposited (for example) by PECVD or with conventional $POCl_3$ diffusion during/following the thermal drive-in step of the boron. Note that the latter can be done in a single high-temperature process step, similar to the co-annealing after ion implantation. However, during the co-annealing step after ion implantation both B and P are already present in the sample, and the applied temperature budget will always affect both dopants. During co-diffusion, on the other hand, the drive-in of boron from the PECVD BSG can be done first (e.g. at 950°C), followed by a P diffusion at a much lower temperature. As a result, P-doped regions with sheet resistances of 80Ω/sq. and surface concentrations of $10^{20}cm^{-3}$ can be achieved. These P diffusions have low saturation current densities and can also be contacted using conventional screen-printed Ag pastes. Co-diffusion from doped oxides therefore seems especially suited to n-PERT BJ solar cells: the PECVD BSG layer may be combined with the rear protection layer, thus not adding to the number of processing steps. Later, P and B can be driven in/diffused during the same high-temperature step (replacing the P diffusion), effectively removing the B diffusion as well as the separate BSG etch from the processing sequence. Ultimately, the n-PERT BJ solar cell would feature the same number of processing steps as for a p-PERC solar cell.

This combination of PECVD BSG as the dopant source and a co-diffusion process was applied to n-PERT BJ solar cells on an area of 239cm². For the first batches, energy conversion efficiencies of up to 19.8% were achieved, with short-circuit current densities J_{sc} of 38.6mA/cm² and open-circuit voltages V_{oc} of 650mV.

Conclusion

By means of two separate quartz furnace diffusions, reference processes were established for bifacial and BJ n-PERT solar cells, yielding efficiencies of up to 20.3% and 20.5% respectively. The n-PERT BJ solar cells were directly compared with p-PERC solar cells, which were fabricated by using the same processing steps and equipment. It was demonstrated that n-PERT BJ solar cells outperform p-PERC solar cells by 0.4% in efficiency after 48 hours of illumination, because of LID of the p-Si. Before LID (or after permanent recovery), p-PERC and n-PERT BJ solar cells achieved similar energy conversion efficiencies.

> "n-PERT BJ solar cells outperform p-PERC solar cells by 0.4% in efficiency after 48 hours of illumination."

The challenge of forming two different full-area highly doped regions can be addressed by employing inherently single-side doping techniques, such as pre-deposition of dopant sources or ion implantation. Both techniques offer specific advantages, in particular with regard to specific cell structures: pre-deposition of dopant sources enables a lean process flow for the fabrication of n-PERT BJ solar cells, while ion implantation is obviously well suited to the fabrication of n-type PERL solar cells. Saturation current densities measured on symmetrical test structures showed that both techniques yield saturation current densities comparable to those obtained in standard quartz furnace diffusions.

Ion implantation and co-annealing have so far been applied to fully screen-printed bifacial n-PERT solar cells, leading to energy conversion efficiencies of up to 20.6%. With PVD Al metallization on the P-doped rear side, efficiencies of up to 20.3% with single screen printing of the AgAl paste, and of up to 20.5% using the dual-print technique on the front side, were achieved. Further investigations into the development of ion-implanted n-PERL solar cells are currently under way. The use of PECVD BSG as a dopant source in combination with a co-diffusion step yielded 19.8% for an n-PERT BJ solar cell.

One should remark that, especially for n-PERT front-junction cells, some technological steps are still less mature than for p-type front-junction cells. In particular, not as much work on optimization has been performed so far on the emitter profile, and screen-print metallization has still to be improved in terms of reduced contact recombination. Given that recent progress continues in these areas, the higher bulk lifetime of n-type material can be expected to yield a higher efficiency benefit in the future.

Outlook

Because an in situ mask can be used to define the processed areas, ion implantation is obviously well suited to the fabrication of n-type PERL solar cells. Implanting phosphorus through a shadow mask, in other words restricting high doping concentrations to the metallized regions, would be beneficial for low specific contact resistances and reduced contact recombination, as well as for reduced Auger and Shockley-Read-Hall surface recombination in the passivated regions. The viability of masked ion implantation has already been demonstrated on p-type solar cells with selective emitters, on ion-implanted IBC cells [19,20], and on n-PERT solar cells with selective boron emitters [17].

Recently, in situ masking of the phosphorus implant was utilized for the fabrication of bifacial n-PERL structures. These structures have so far exhibited efficiencies comparable to those obtained for the n-PERT references. In order to exploit the full efficiency potential of the n-PERL structure, further optimization will be necessary.

Acknowledgements

We thank M. Berger, A. Christ, S. Kirstein, S. Spätlich, B. Gehring, P. Giesel and A. Klatt for their help with sample processing, R. Brendel for continuous support, and M. Emsley and J. Graff for valuable discussions. This work was funded by the German Federal Ministry for Economic Affairs and Energy under Grant 0325478 (SimpliHigh) and under Grant 0325480 (CHIP), as well as by Applied Materials/Varian.

References

[1] SEMI PV Group Europe 2014, "International technology roadmap for photovoltaic (ITRVP): Results 2013", 5th edn (March) [http://www.itrpv.net/Reports/Downloads/].

[2] Schmidt, J., Aberle, A.G. & Hezel, R. 1997, "Investigation of carrier lifetime instabilities in Cz-grown silicon", *Proc. 26th IEEE PVSC*, Anaheim, California, USA, p. 13.

[3] Schmidt, J. et al. 2007, "n-type silicon – The better material choice for industrial high-efficiency solar cells?", *Proc. 22nd EU PVSEC*, Milan, Italy, p. 998.

[4] Smith, D.D. et al. 2013, "SunPower's Maxeon Gen III solar cell: High efficiency and energy yield", *Proc. 39th IEEE PVSC*, Tampa, Florida, USA, pp. 0908–0913.

[5] Taguchi, M. et al. 2014, "24.7% record efficiency HIT solar cell on thin silicon wafer", *IEEE J. Photovolt.*, Vol. 4, No. 1, pp. 96–99.

[6] Benick, J. et al. 2014, "High efficiency n-type PERT and PERL solar cells", *Proc. 40th IEEE PVSC*, Denver, Colorado, USA.

[7] Song, D. et al. 2012, "Progress in n-type Si solar cell and module technology for high efficiency and low cost", *Proc. 38th IEEE PVSC*, Austin, Texas, USA, pp. 003004–003008.

[8] Romijn, I.G. et al. 2013, "Industrial cost effective n-PASHA solar cells with >20% efficiency", *Proc. 28th EU PVSEC*, Paris, France, pp. 736–740.

[9] Gall, S. et al. 2013, "High efficient industrial n-type technology: From cell to module", *Proc. 28th EU PVSEC*, Paris, France, pp. 695–698.

[10] Böschke, T.S. et al. 2014, "Fully Ion Implanted n-type Cells – A Contender for Industrial Cells with >20.5% Efficiency", *IEEE J. Photovolt.*, Vol. 4, No. 1, pp. 48–51.

[11] Ok, Y.-W. et al. 2014, "Ion-implanted and screen-printed large area 20% efficient n-type front junction Si solar cells", *Solar Energy Mater. & Solar Cells*, Vol. 123, pp. 92–96.

[12] Kiefer, F. et al. 2014, "Influence of the boron emitter profile on V_{oc} and JSC losses in fully ion implanted n-type PERT solar cells", *physica status solidi (a)*, 10.1002/pssa.201431118.

[13] Edler, A. et al. 2012, "Metal induced losses in bifacial n-type silicon solar cells: Investigation in simulation and experiment", *Proc. 22nd EU PVSEC*, Milan, Italy.

[14] Mertens, V. et al. 2013, "Large area n-type Cz double side contact back junction solar cell with 21.3% conversion efficiency", *Proc. 28th EU PVSEC*, Paris, France, pp. 714–717.

[15] Hannebauer, H. et al. 2014, "21.2%-efficient fineline-printed PERC solar cell with 5 busbar front grid", *physica status solidi (RRL)*, Vol. 8, No. 8, pp. 675–679.

[16] Lim, B. et al. 2014, "n-PERT back junction solar cells: An option for the next industrial technology

generation?", *Proc. 29th EU PVSEC*, Amsterdam, The Netherlands.
[17] Kiefer, F. et al. 2014, "Emitter recombination current densities of boron emitters with silver/aluminum pastes", *Proc. 40th IEEE PVSC*, Denver, Colorado, USA.
[18] Benick, J. et al. 2010, "Very low emitter saturation current densities on ion implanted boron emitters", *Proc. 25th EU PVSEC*, Valencia, Spain, pp. 1169–1173.
[19] Mo, C.B. et al. 2012, "High efficiency back contact solar cell via ion implantation", *Proc. 27th EU PVSEC*, Frankfurt, Germany.
[20] BOSCH Solar Energy 2013, Press release (August 15th) [www.solarserver.de, www.pv-magazine.de].
[21] Krügener, J. et al. 2014, "Electrical and structural analysis of crystal defects after high-temperature rapid thermal annealing of highly boron ion-implanted emitters", submitted to *IEEE J. Photovolt.*
[22] Richter, A., Benick, J. & Hermle, M. 2013, "Boron emitter passivation with Al_2O_3 and Al_2O_3/SiN_x stacks using ALD Al_2O_3", *IEEE J. Photovolt.*, Vol. 3, No. 1, pp. 236–245.
[23] Edler, A. et al. 2014, "Metallization-induced recombination losses of bifacial silicon solar cells", *Prog. Photovolt.: Res. Appl.*, DOI: 10.1002/pip.2479.
[24] Katkhouda, K. et al. 2014, "Aluminum-based rear-side PVD metallization for nPERT silicon solar cells", *IEEE J. Photovolt.*, Vol. 4, No. 1, pp. 160–167.
[25] Barth, S. et al. 2013, "19.4 efficient bifacial solar cell with spin-on boron diffusion", *Energy Procedia*, Vol. 38, pp. 410–415.
[26] Aleman, M. et al. 2012, "Development and integration of a high efficiency baseline leading to 23% IBC cells", *Energy Procedia*, Vol. 27, pp. 638–645.
[27] Rothhardt, P. et al. 2013, "Co-diffusion from solid sources for bifacial n-type silicon solar cells", *physica status solidi (RRL)*, Vol. 7, No. 9, pp. 623–626.
[28] Rothhardt, P. et al. 2014, "19.9% efficient bifacial n-type solar cell produced by co-diffusion-cobin", *Proc. 29th EU PVSEC*, Amsterdam, The Netherlands, pp. 653–655.
[29] Wehmeier, N. et al. 2013, "Boron-doped PECVD silicon oxides as diffusion sources for simplified high-efficiency solar cell fabrication", *Proc. 28th EU PVSEC*, Paris, France, pp. 1980–1984.

About the Authors

Bianca Lim studied physics at Freie Universität Berlin and did her diploma thesis at Hahn-Meitner-Institut Berlin. She then joined ISFH to pursue a doctorate, focusing on boron-oxygen-related recombination centres in silicon, and was awarded a Ph.D. (Dr. rer. nat.) by the Leibniz University of Hanover in 2011. She is currently a project leader at ISFH, working on simplified processes for local doping and n-type PERT silicon solar cells.

Fabian Kiefer received a diploma degree in physics from the University of Freiburg, Germany, in 2010 for his research on epitaxially grown emitters on crystalline silicon solar cells and on crystalline silicon thin-film solar cells, carried out at the Fraunhofer Institute for Solar Energy Systems (ISE) in Freiburg. In 2010 he joined ISFH, where he is working towards his Ph.D. His research focuses on boron emitters for n-type silicon solar cells.

Nadine Wehmeier has been a Ph.D. student since 2012 at the Institute for Solar Energy Research Hamelin (ISFH), where she works on PECVD doped oxide layers as diffusion sources and co-diffusion processes. She studied physics at the University of Münster and received her M.Sc. in 2011 for her work on silicon multilayer structures for thermoelectric applications.

Till Brendemühl received his diploma degree in engineering physics from the University of Applied Sciences in Emden, Germany. He has been with ISFH since 2005, first working on laser processes and later becoming a project leader with a focus on back-contact high-efficiency solar cells. He is currently working on screen-printed n-PERT solar cells in the solar cell production processes group.

Yevgeniya Larionova studied physics and received her Ph.D. in optics (laser physics) from V.N. Karazin Kharkov National University in Ukraine. From 2002 to 2007 she worked as a research scientist in the Optics Department at Physikalisch-Technische Bundesanstalt (PTB, Braunschweig, Germany). She has been a research scientist at ISFH since 2007.

Frank Heinemeyer studied mineralogy at the Leibniz University of Hanover and received his diploma degree in 1997 on selenization of galvanic-deposited CuIn-layers for $CuInSe_2$ solar cells. He joined ISFH in 2001, working on CIGS solar cells on textile fibres. Since 2007 he has been a project leader in the process technology group, with a focus on the metallization of crystalline silicon solar cells.

Jan Krügener received his diploma and Ph.D. degrees in electrical engineering from the Leibniz University of Hanover, where he is currently an associate researcher in the Institute of Electronic Materials and Devices. His research focuses on the fabrication and characterization of advanced high-efficiency silicon solar cells.

Robby Peibst received his diploma degree in technical physics in 2005 from the Ilmenau University of Technology in Germany. In 2010 he received his Ph.D. from the Leibniz University of Hanover, with a thesis involving germanium-nanocrystal-based memory devices. He joined ISFH in 2010 and has led the emerging c-Si technologies group since 2013. His research focuses on techniques for producing high-efficiency silicon solar cells.

Thorsten Dullweber received his Ph.D. from the University of Stuttgart in 2002. From 2001 to 2009 he worked as a microelectronics project leader at Siemens, Infineon and Qimonda. Since 2009 he has led the ISFH R&D solar cell production processes group, focusing on process and efficiency improvements in industrial-type screen-printed silicon solar cells.

Enquiries

Bianca Lim
Institut für Solarenergieforschung Hameln (ISFH)
D-31860 Emmerthal
Germany

Email: lim@isfh.de
Website: www.isfh.de